Photoacoustics 3 (2015) 45–54

Contents lists available at ScienceDirect

Photoacoustics

journal homepage: www.elsevier.com/locate/pacs

Research Article

Photoacoustic imaging driven by an interstitial irradiation source

Trevor Mitcham [a,c], Katherine Dextraze [a,c], Houra Taghavi [a], Marites Melancon [b,c], Richard Bouchard [a,c]

[a] Department of Imaging Physics, University of Texas MD Anderson Cancer Center, Houston, TX 77030, USA
[b] Department of Interventional Radiology, University of Texas MD Anderson Cancer Center, Houston, TX 77030, USA
[c] Graduate School of Biomedical Sciences, University of Texas at Houston, Houston, TX 77030, USA

ARTICLE INFO

Article history:
Received 9 July 2014
Received in revised form 20 December 2014
Accepted 16 February 2015
Available online 14 March 2015

Keywords:
Photoacoustic imaging
Interstitial source
Optical fiber
Multi-wavelength imaging
Improved penetration depth
Interventional radiology

ABSTRACT

Photoacoustic (PA) imaging has shown tremendous promise in providing valuable diagnostic and therapy-monitoring information in select clinical procedures. Many of these pursued applications, however, have been relatively superficial due to difficulties with delivering light deep into tissue. To address this limitation, this work investigates generating a PA image using an interstitial irradiation source with a clinical ultrasound (US) system, which was shown to yield improved PA signal quality at distances beyond 13 mm and to provide improved spectral fidelity. Additionally, interstitially driven multi-wavelength PA imaging was able to provide accurate spectra of gold nanoshells and deoxyhemoglobin in excised prostate and liver tissue, respectively, and allowed for clear visualization of a wire at 7 cm in excised liver. This work demonstrates the potential of using a local irradiation source to extend the depth capabilities of future PA imaging techniques for minimally invasive interventional radiology procedures.

1. Introduction

In the past twenty years, image guidance has been utilized increasingly to improve the precision and efficacy of diagnostic and therapeutic procedures [1]. Typically, image guidance is provided by ultrasound (US), X-ray computed tomography, fluoroscopy, or magnetic resonance imaging. Photoacoustic (PA) imaging is a promising technique that is non-ionizing, low-cost, and offers high-contrast imaging of both the surgical tools and photoabsorbers that are often encountered in diagnostic and therapeutic techniques. To provide accurate guidance, PA images can be co-registered with US imaging to generate a photoacoustic-ultrasonic (PAUS) image that contains clear anatomical information and provides high-contrast visualization of important photoabsorbers, such as hemoglobin or targeted nanoparticles [2]. To date, however, the application of PAUS imaging has typically been limited to superficial anatomical sites due to the relatively shallow penetration depth of the external irradiation source.

PA imaging requires a narrow-pulse-width laser irradiation source, photoabsorbers to generate PA-induced pressure waves, and an US transducer for signal detection. The light provided by the pulsed irradiation source is absorbed by photoabsorbers and immediately converted to heat. This thermal transient leads to rapid local expansion, creating pressure waves that can be detected with high spatiotemporal resolution by an US transducer. The resulting pressure waves are dependent on local fluence, optical absorption, and thermally dependent material properties [3]. The initial local pressure (p_0) generated by the PA effect can be described as

$$p_o = \frac{\beta c^2}{C_p}\mu_a F = \Gamma A, \tag{1}$$

where $\beta[\frac{1}{K}]$ is the thermal coefficient of volume expansion, $c[\frac{m}{s}]$ is the speed of sound through tissue, $C_p[\frac{J}{K\cdot kg}]$ is the heat capacity at constant pressure, $\mu_a[\frac{1}{cm}]$ is the optical absorption coefficient, $F[\frac{J}{cm^2}]$ is the local laser fluence, Γ is the Grüneisen coefficient, and $A[\frac{J}{cm^3}]$ is the local deposition energy.

As laser light travels through a medium (e.g., tissue), fluence is lost due to optical scattering and absorption by tissue components like blood and adipose tissue. This fluence loss is the primary cause of the limited depth penetration that has previously hindered the clinical application of PA imaging. Compensating for fluence loss is a nuanced problem. The laser fluence applied to skin in clinical applications is regulated by the American National Standards Institute (ANSI), which recommends that clinical skin exposure to low near-infrared (NIR) light not exceed specific fluence levels

E-mail address: rrbouchard@mdanderson.org.

http://dx.doi.org/10.1016/j.pacs.2015.02.002

ranging from 20 $\frac{mJ}{cm^2}$ at 700 nm, to 50 $\frac{mJ}{cm^2}$ at 900 nm, to 100 $\frac{mJ}{cm^2}$ at 1050 nm [4,5]. Therefore, depth penetration cannot be improved by simply increasing surface fluence. Previous work has explored using a 1064-nm wavelength laser for PA imaging applications. At this wavelength, tissue scattering and absorption is decreased compared to lower NIR wavelengths, while the exposure limitations through skin rise linearly to 100 $\frac{mJ}{cm^2}$, providing a situation in which more laser light can be delivered to target photoabsorbers [4–6]. The reduction in tissue scattering and absorption at 1064 nm also results in reduced background signal in PA images, which improves the contrast of the images compared to imaging at lower wavelengths in the NIR range [7]. However, the depth penetration with 1064-nm irradiation can still be quite limited for clinical applications, and such an implementation can restrict opportunities for multi-wavelength imaging. One final method to improve imaging depth is to fundamentally change the absorption properties of the target being imaged, a technique that has been demonstrated for metallic objects [8].

To circumvent the depth penetration limitation of NIR irradiation, endoscopic, intravascular and transrectal PA imaging techniques have been developed for targeting deeper tissues [9–14]. Although these techniques have been effective for imaging particular structures, such as the prostate, colon, or vascular wall, they have not been applied more generally to deep-tissue imaging. Furthermore, the smaller US transducers that are used to accommodate PA endoscopic or intravascular imaging have lower sensitivity and a reduced receive-aperture extent (compared to larger, more conventional US arrays), resulting in reduced image quality [15]. Therefore, in order to deliver light to deep tissues while maintaining image quality, an interstitial optical source could be introduced to provide local irradiation of the target, while a conventional diagnostic US array could be used for external acoustic detection and PA image formation.

This work investigated the use of a single interstitial optical fiber co-registered with an external US transducer to provide PA images for specific interventional radiology (IR) procedures (e.g., laser ablation or biopsy guidance). Optical fibers were modified to serve as a local, interstitial irradiation source. To demonstrate initial feasibility of the interstitial PA imaging system, wire targets, gold nanoshells (AuNSs), and deoxyhemoglobin were imaged in tissue-mimicking phantoms and in ex-vivo tissue.

2. Materials and methods

2.1. General setup and fiber processing

The imaging setup consisted of a pulsed laser source that triggered the receive acquisition of a clinical US system. A Quanta-Ray® PRO pulsed Nd:YAG laser coupled into a tunable GWU versaScan optical parametric oscillator (OPO; Newport Corp., Irvine, CA) was used to provide pulsed NIR irradiation. After exiting the OPO, the beam was sent through a neutral-density filter to a plano-convex focusing lens (Thorlabs Inc., Newton, NJ) that adjusted the spot size to allow for better coupling into optical fibers with a 1000-μm diameter. This diameter was chosen because it coincides with the size of needles often used in biopsy procedures, providing more clinically relevant implantation of the fiber into the tested phantoms [16]. After the focusing lens, a custom-built fiber holder was connected to a three-dimensional micrometer-driven platform to allow for precision translation of the fiber coupling stage (MBT616D; Thorlabs Inc., Newton, NJ). From the coupling stage, the fiber was inserted into a phantom and used to generate a PA signal that was detected with a Vantage 128 US system using an L11-4v linear array operating at 6.25 MHz (Verasonics, Inc., Redmond, WA). A schematic of the complete system setup is provided in Fig. 1. Pulse energy readings were taken with a Nova II meter connected to a PE50-DIF-ER-V2 detector with diffuser (Ophir Optronics Solutions Ltd., Jerusalem, Israel) while laser wavelength was calibrated using a Thorlabs CCS175 compact spectrometer (Thorlabs Inc., Newton, NJ). Energy delivery to the fiber was estimated by splitting the primary beam into the energy meter using a glass slide. The energy meter was also placed at the irradiating side of each fiber prior to a study to determine the wavelength-dependent ratio between measured input energy and output energy. This ratio and the estimated input energy values obtained from the beam splitter were utilized to normalize for output fluence differences between wavelengths. Additionally, laser spot size measurements were taken by coupling a continuous wave (CW) laser into the fiber and measuring the projected spot at 5 mm from the fiber tip.

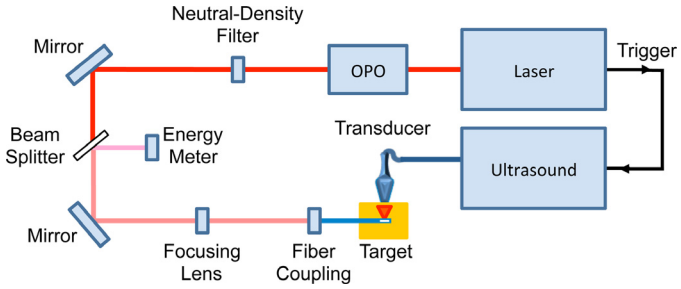

Fig. 1. Schematic of PA imaging system driven by an interstitial irradiation source.

Two different types of 1000-μm-diameter fibers were used in this study. All but one study utilized custom-built, side-fire 1000-μm fibers (Fig. 2.d; Thorlabs Inc., Newton, NJ). In order for optical fibers to transmit light efficiently, both the proximal (i.e., the end coupled to the incoming laser beam) and distal (i.e., the end acting as a local optical source) ends of the fiber must be beveled to appropriate angles and minimized of surface imperfections [12]. Proximal ends were left flat, polished, then qualitatively inspected using a digital microscope (zipScope; Aven Inc., Ann Arbor, MI,) to ensure surface smoothness (Fig. 2.b-c). If any scratches or cloudy areas were present, the polishing sequence was repeated until the surface appeared visually smooth. Upon completion of the proximal fiber tip, the distal tip was sanded using a custom-built, angled sanding apparatus (Fig. 2.a) until the tip was beveled to a critical angle of 35°; it was then polished in a similar fashion to the procedure implemented for the proximal tip. The distal tip was beveled to promote total internal reflection, which allows the fiber to emit light perpendicularly (i.e., side-fire) rather than out the tip (i.e., straight-fire) [12]. As the coupling medium at the end of the fiber determines the critical angle needed, quartz end-caps were added (Sutter Instrument Co., Novato, CA) to ensure that the fiber tip was always air-backed. The spot size 5 mm lateral from the tip was measured to be approximately 0.2 cm^2. Side-fire fibers were implemented in the majority of the studies as they could be readily produced in-house and they tended to provide increased fluence in their limited irradiation volume.

The last study utilized a clinically-approved fiber with a conical distal tip that provided 360° irradiation from a 35° half angle at the distal tip with a spot size of 2.5 cm^2 (i.e., 3.1 cm circumference and 0.8 cm height) at a lateral distance of 5 mm (Fig. 2.e; Pioneer Optics Co., Bloomfield, CT); this fiber is typically used for administration of photodynamic therapy.

All tissue-mimicking phantoms used in this investigation were created using 8% (wt%) gelatin (Sigma-Aldrich Co., St. Louis, MO), 5% Intralipid® (Sigma-Aldrich, St. Louis, MO), 1% silica (US Silica, Frederick, MD), 0.1% formaldehyde (Sigma-Aldrich Corp., St. Louis, MO), and 85.9% deionized (DI) H_2O in order to generally mimic the